New Phytologist

Research

The *Hebeloma cylindrosporum* HcPT2 Pi transporter plays a key role in ectomycorrhizal symbiosis

Adeline Becquer[1]*, Kevin Garcia[2,3]*, Laurie Amenc[1], Camille Rivard[4,5], Jeanne Doré[6], Carlos Trives-Segura[1], Wojciech Szponarski[3], Sylvie Russet[1], Yoan Baeza[1], Benedikt Lassalle-Kaiser[5], Gilles Gay[6], Sabine Dagmar Zimmermann[3] and Claude Plassard[1]

[1]Eco & Sols, Université de Montpellier, CIRAD, INRA, IRD, Montpellier SupAgro, 34060 Montpellier, France; [2]Department of Biology and Microbiology, South Dakota State University, Brookings, SD 57007, USA; [3]BPMP, Université de Montpellier, CNRS, INRA, SupAgro, 34060 Montpellier, France; [4]CEPIA, INRA, 44300 Nantes, France; [5]Synchrotron SOLEIL, 91190, Gif-sur-Yvette, France; [6]LEM, CNRS, INRA, VetAgro Sup, UCBL, Université de Lyon, 69622 Villeurbanne, France

Author for correspondence:
Claude Plassard
Tel: +33 499 612 979
Email: claude.plassard@inra.fr

Received: *26 April 2018*
Accepted: *28 May 2018*

New Phytologist (2018)
doi: 10.1111/nph.15281

Key words: ectomycorrhizal (ECM) fungus, overexpression, ^{32}P labeling, phosphate transporter, *Pinus pinaster*, RNA interference, X-ray fluorescence mapping.

Summary

- Through a mutualistic relationship with woody plant roots, ectomycorrhizal fungi provide growth-limiting nutrients, including inorganic phosphate (Pi), to their host. Reciprocal trades occur at the Hartig net, which is the symbiotic interface of ectomycorrhizas where the two partners are symplasmically isolated. Fungal Pi must be exported to the symbiotic interface, but the proteins facilitating this transfer are unknown.
- In the present study, we combined transcriptomic, microscopy, whole plant physiology, X-ray fluorescence mapping, ^{32}P labeling and fungal genetic approaches to unravel the role of HcPT2, a fungal Pi transporter, during the *Hebeloma cylindrosporum–Pinus pinaster* ectomycorrhizal association.
- We localized HcPT2 in the extra-radical hyphae and the Hartig net and demonstrated its determinant role for both the establishment of ectomycorrhizas and Pi allocation towards *P. pinaster*. We showed that the host plant induces *HcPT2* expression and that the artificial overexpression of *HcPT2* is sufficient to significantly enhance Pi export towards the central cylinder.
- Together, our results reveal that HcPT2 plays an important role in ectomycorrhizal symbiosis, affecting both Pi influx in the mycelium and efflux towards roots under the control of *P. pinaster*.

Introduction

Plant growth and development are highly dependent on nutrient availability in the rhizosphere, which is often a limiting factor. As a consequence, land plants have evolved various strategies to optimize nutrient acquisition, including beneficial interactions with soil-borne microbes. In northern hemisphere forests, ectomycorrhizal (ECM) associations play a determinant role in tree nutrition. These mutualistic associations between the roots of woody plants and filamentous fungi optimize water and nutrient acquisition for both partners (Garcia *et al.*, 2016).

ECM fungi take up macronutrients from the soil and transport them towards the host plant in exchange for photosynthesis-derived carbohydrates (Smith & Read, 2008). These reciprocal trades take place at the symbiotic interface of ectomycorrhizas, in a specific fungal structure developing between root cortical cells called the Hartig net.

Phosphorus (P) is one of the most essential macronutrients for plant growth and productivity, and participates to many biological processes, such as energy metabolism, signalization and photosynthesis (Raghothama, 1999; Vance *et al.*, 2003). Free concentrations of inorganic orthophosphate (Pi) in the soil, which is the only form of P directly available for plants, are very low, ranging from 1 to 10 μM (Hinsinger, 2001). This low availability is due to the rapid sequestration of Pi negative charges by free cations (Hinsinger, 2001; Vance *et al.*, 2003). As a consequence, Pi uptake generates large depletion zones around the roots, decreasing its availability for the plant.

Plants colonized by ECM fungi gain access to a larger surface of soil than noncolonized ones, far beyond depletion zones, via the extra-radical mycelium of the fungal partner (Smith & Read, 2008; Plassard & Dell, 2010; Cairney, 2011; Smith *et al.*, 2015). Pioneer studies using radiotracers demonstrated the transport of ^{32}Pi from extra-radical hyphae towards the plant cells, through the Hartig net (Melin & Nilsson, 1950). More specifically, ECM fungi express several high-affinity transporters in extra-radical hyphae to acquire Pi from the soil (Tatry *et al.*, 2009; Casieri *et al.*, 2013; Becquer *et al.*, 2014; Courty *et al.*, 2016; Garcia *et al.*, 2016). Once acquired, Pi is accumulated in fungal vacuoles

*These authors contributed equally to the work.

as polyphosphates (polyPs) (Ashford *et al.*, 1994, 1999). Early experiments using radioactive isotopes revealed that polyPs may contain *c.* 90% of the total P taken up by ectomycorrhizas (Harley, 1978). PolyPs are then translocated via a motile tubular vacuolar system (Ashford & Allaway, 2002) before being hydrolyzed within the Hartig net (Cairney, 2011). This provides Pi efflux from fungal cells to the interfacial apoplast (Torres-Aquino *et al.*, 2017). Finally, Pi is taken up by, as yet, uncharacterized plant transporters that are specifically up-regulated in colonized roots (Loth-Pereda *et al.*, 2011; Kariman *et al.*, 2014). Although we have known for over half a century that ECM fungi play a crucial role in Pi nutrition of trees, the molecular mechanisms underlying fungal Pi secretion towards the plant root cells remain largely unknown.

Two main types of high-affinity P transporters have been characterized in the model fungus *Saccharomyces cerevisiae* that are Pi:Na^+ (ScPho89) and H^+:Pi (ScPho84) symporters (Bun-ya *et al.*, 1991; Martinez & Persson, 1998). The search for homologous genes in available genomes of ECM fungi shows that the vast majority of Basidiomycete species display only H^+:Pi symporters, contrary to the Ascomycete *Tuber melanosporum*, which harbors both Pi:Na^+ and H^+:Pi symporters (Casieri *et al.*, 2013; Hacquard *et al.*, 2013; Nehls & Plassard, 2018). To date, only two P transporters from *Hebeloma cylindrosporum* (HcPT1.1 and HcPT2), one from *Boletus edulis* (BePT), one from *Rhizopogon luteolus* (RlPT) and one from *Leucocortinarius bulbiger* (LbPT) have been characterized as high-affinity H^+:Pi transporters (Tatry *et al.*, 2009; Wang *et al.*, 2014; Zheng *et al.*, 2016). Recent analysis of the *H. cylindrosporum* genome revealed another putative H^+:Pi transporter closely related to HcPT1.1 and called HcPT1.2 (Casieri *et al.*, 2013; Kohler *et al.*, 2015). The immunolocalization of HcPT1.1 revealed its presence in extra-radical hyphae, fungal mantle and Hartig net of ectomycorrhizas (Garcia *et al.*, 2013). Regarding HcPT2, transcripts were predominantly detected in ectomycorrhizas under both high and low P availability but also in extra-radical hyphae (Tatry *et al.*, 2009). Hence, we hypothesized that this transporter may play a key role in the ectomycorrhizal symbiosis regarding fungal Pi uptake and delivery to the host plant *Pinus pinaster*.

In the present study, we show that, among the three *H. cylindrosporum* genes encoding H^+:Pi transporters, *HcPT2* is the only one whose transcription is strongly up-regulated in ectomycorrhizas compared to free-living mycelium. To understand its role further, we localized the protein in ectomycorrhizas and used transgenic fungal lines under- or over-expressing *HcPT2* to quantify their effects on mycorrhizal intensity, whole plant P accumulation and P accumulation in ectomycorrhizas using X-ray fluorescence mapping. We also used ^{32}P labeling of mycelia to follow its fate towards the host plant.

Materials and Methods

Plant and fungal material

The wild-type homokaryotic strain h7 of the ECM basidiomycete *H. cylindrosporum* Romagnesi (Debaud & Gay, 1987) was used for agrotransformation as described previously (Combier *et al.*, 2003; Garcia *et al.*, 2013). Among the 15 carboxin-resistant transgenic lines down-regulating (RNAi) or overexpressing (OE) *HcPT2*, two independent isolates per transgenic line (RNAi-PT2-6, RNAi-PT2-9 and OE-PT2-4, OE-PT2-7) were used in this work. 'Ctl' refers to the wild-type strain expressing an empty vector (Garcia *et al.*, 2014).

Fungal cultures were grown in the dark at 25°C, either on solid YMG medium (Rao & Niederpruem, 1969) or in a complete nutrient solution (+P) containing 1 mM Pi (see Supporting Information Methods S1). Two-week-old liquid cultures were used to examine fungal growth and gene expression, or to initiate new axenic cultures for the experiment mimicking the symbiotic interface without physical contact (see 'Symbiotic interface-mimicking experiment').

Surface sterilized maritime pine seedlings (*P. pinaster* Soland in Ait. from the Médoc, Landes-Sore-Vergé source) were grown first in test tubes, left uninoculated or inoculated with 3-wk-old wild-type or transgenic fungi as described previously (Plassard *et al.*, 1994; Garcia *et al.*, 2014). Mycorrhizal and nonmycorrhizal (NM) plants were watered every week with 15 ml of mineral nutrient solution (Torres-Aquino *et al.*, 2017). All test tubes were placed in a growth chamber under a 16 h : 8 h, light–dark cycle at 25°C/20°C, 80%/100% relative humidity, CO_2 concentration of *c.* 350×10^{-6} $dm^3\,dm^{-3}$ and a photosynthetically active radiation (PAR) of *c.* 400 $\mu mol\,m^{-2}\,s^{-1}$ (400–700 nm). Two-month-old plants were used for ECM assays, elemental P mapping and symbiotic interface-mimicking experiments.

Ectomycorrhizal assays in Petri dishes

Plants were transferred to sterile 12 × 12 cm Petri dishes with the shoot outside the plate. Each Petri dish was filled with 20 g of equal parts chromic cambisol (Cazevielle, Herault, France; Casarin *et al.*, 2004) and sand (Sigma-Aldrich) (1 : 1, w/w) and sterilized twice (120°C, 20 min). The soil was used either without any treatment (bicarbonate-extractable Pi content of 3 mg kg^{-1}; −P soil) or after addition of soluble Pi (310 mg P kg^{-1} dry soil supplied as KH_2PO_4; +P soil) as described by Casarin *et al.* (2004). The root system was placed on the surface of the soil layer and the plates were sealed and placed for 70 d in the growth chamber (as described above). Plants were watered once a week with sterile P-free solution to maintain the moisture level. At harvest, total P in shoots and roots was determined. In total, there were 14 combinations in this study: seven associations (NM, h7, Ctl, OE-PT2-4, OE-PT2-7, RNAi-PT2-6 and RNAi-PT2-9) with two different Pi supplies, and six replicates per treatment. Petri dishes were randomized and rotated weekly. The experiment was repeated twice independently.

Elemental P mapping using X-ray fluorescence

Root systems from plants in test tubes were rinsed with demineralized water. Short roots were cut under a stereomicroscope, embedded in a cryo-protectant and immediately plunged into isopentane cooled by liquid N_2 to cryo-fix the cells and their

contents. Cryo-thin sections of 20 µm were prepared using a cryotome and analyzed at the SOLEIL synchrotron facility using the microfocused LUCIA beamline (Vantelon *et al.*, 2016). Samples were set on an N_2-cooled cryostage, which was moved relative to the focused beam at 3.7 keV to collect the X-ray fluorescence spectra within each pixel (3 × 3 µm) over the zone of interest. Phosphorous X-ray fluorescence maps were plotted after X-ray fluorescence spectra fitting using the PYMCA software (Solé *et al.*, 2007). All the pixels corresponding to different cellular territories (e.g. root cortex vs central cylinder and cytosol vs vacuole in cortex) were then selected using data filtering with threshold values deduced from linear plots traced through each map (see Fig. S1 and Methods S1). For each root type, data were extracted from three sections obtained from two plants.

Symbiotic interface-mimicking experiment

Twelve-day-old +P fungal cultures were grown for seven additional days in −P solution to get P-starved mycelia. They were transferred for 16 h into the +P solution and labeled with ^{32}P or left unlabeled (for details, see Methods S1; Becquer *et al.*, 2017; Torres-Aquino *et al.*, 2017). In this set of experiments, plant roots and the fungus were incubated for up to 48 h in the same interaction medium (without P and C source, buffered pH of 5.9) mimicking the symbiotic interface of the Hartig net. The experimental set-up consisted of plastic syringes filled with 60 ml of interaction medium constantly air-aerated and receiving either one mycelium only ('no plant' condition) or one mycelium along with three seedlings ('with *P. pinaster*' condition) (see Methods S1 for details). The experiment was performed using ^{32}P-labeled mycelia for all transgenic lines (Ctl, OE-PT2-4, OE-PT2-7, RNAi-PT2-6 and RNAi-PT2-9). The total number of syringes was 60, corresponding to two conditions, one final sampling time, five fungal strains and six replicates. At 48 h, mycelia and plants were harvested and the fresh weight was recorded. The volume of induction medium from each syringe was also recorded. Measurements of ^{32}P in labeling solution, induction medium, mycelia and plants were carried out as detailed in Methods S1.

Total P determination

Root and shoot tissues were dried at 60°C for 2 d, weighed and ground. Ten milligrams was mineralized in H_2SO_4 (36 N) at 330°C for 10 min as described by Ali *et al.* (2009). Total P concentrations were determined using the Malachite Green method (Ohno & Zibilske, 1991).

Plasmid construction for localization and functional analyses of HcPT2

A vector containing the *HcPT2–EGFP* chimeric construct under the control of the *HcPT2* promoter region (1068 bp) was used for the localization of HcPT2 proteins in ectomycorrhizas. The resulting vector, pPZP-PPT2-PT2::E, was constructed using the pPZP-Pgpd-E plasmid as explained previously (Garcia *et al.*, 2013, 2014). Two independent isolates (HcPT2-EGFP-1 and HcPT2-EGFP-5) were used for HcPT2 localization.

To overexpress *HcPT2* in the fungus, a pPZP-OE-PT2 vector was constructed. The coding sequence of *HcPT2* was amplified from cDNA contained in the pFL61 vector (Tatry *et al.*, 2009) using specific primers (Table S1), and inserted in the final pPZP-P-T vector derived from pPZP-133 harboring a carboxin resistance cassette (Fig. S2; Ngari *et al.*, 2009). To down-regulate *HcPT2* in the fungus, sense and antisense 300 bp cDNA fragments were amplified using specific primers (Table S1) and cloned using *Sna*BI/*Hin*dIII sites (sense) and *Kpn*I/*Sph*I sites (antisense) into the pSILBAγ vector (Kemppainen & Pardo, 2010). The entire silencing cassette was removed from pSILBAγ using *Xba*I restriction enzyme and inserted into pPZP-133 to form the final pPZP-RNAi-PT2 vector.

Cellular and sub-cellular localization of HcPT2

Immunolocalizations were performed on ectomycorrhizas from plants grown for 2.5 months in mini-rhizoboxes filled with +P or −P soil (Casarin *et al.*, 2004). Antibodies in chicken (https://www.genosphere-biotech.com) were raised against a 16 amino acid peptide of the N-terminal region of HcPT2 (5′-GDDIEELKKAQKAEEC-3′) predicted to be outside of the plasma membrane, in the cytosol, and their specificity was checked using western-blots (Fig. S3, see Methods S1). The antibodies were diluted at 1 : 1000 (6 µg ml^{-1}). Longitudinal or radial 7 µm sections were prepared from ectomycorrhizas from five plants (see Methods S1) and incubated overnight at 4°C with anti-HcPT2 antibody in PBS with 4% BSA. After washing, sections were incubated for 1 h under dark conditions in 4% PBS-BSA containing the goat anti-chicken IgG-Dylight 405 conjugates (Jackson ImmunoResearch Inc, West Grove, PA, USA) (5 µg ml^{-1}), as a secondary antibody. Sections were mounted in Mowiol 4.88 and analyzed by confocal microscopy (Zeiss LSM 780, with a Plan-Apochromat 40×/1.3 oil objective, Montpellier RIO Imaging platform). For excitation and fluorescence detection, a channel spectral laser set at 405 nm and a 420–480 nm emission band-pass were used. Cell wall autofluorescence was acquired at 555 nm/530–600 nm (excitation/emission wavelengths). Images were analyzed with Zeiss ZEN BLACK software.

For transmission electron microscopy, ectomycorrhizas were prepared according to the classical Tokuyasu technique for immunogold-labeling (Peters *et al.*, 2006). Briefly, cells were fixed overnight in 0.2% (v/v) glutaraldehyde and 2% formaldehyde in PBS, embedded in 12% gelatin (type A, bloom 300; Sigma), cryo-sectioned with a diamond knife using a Leica (Wetzlar, Germany) EM FC7 ultramicrotome, and mounted on copper grids. Immunogold labeling was performed on thin sections using anti-HcPT2 antibodies diluted in PBS (1 : 1000) and goat anti-chicken IgG attached to 25 nm gold particles (Aurion, Wageningen, the Netherlands). Images were taken using a Tecnai G20 transmission electron microscope operating at 200 kV (FEI company, Hillsboro, OR, USA). Samples with the primary antibody omitted were used as labeling-specificity controls.

Determination of ectomycorrhizal phenotype

Ectomycorrhizas were produced in 12 × 12 cm Petri dishes as described by Combier *et al.* (2004). Two-week-old *P. pinaster* seedlings were placed on solid modified Melin-Norkrans medium (Norkrans, 1949) supplemented with glucose (2.7 mM). Plants were inoculated with fungal plugs and placed along the primary root. The presence of ectomycorrhizas was determined after 4 wk using stereomicroscopy (Wild Makroscop M420; Leica Microsystemes SAS, Nanterre, France). Images were taken with a camera (Leica DFC320) and the software from Leica Application Suite, v.4.8.0. In parallel, relative root colonization was determined using ImageJ software (http://imagej.nih.gov/ij/) applied to images taken from plants roots grown in soil (see ECM assays). Relative fungal growth area was determined by the visible fungal growth area compared to the total Petri dish area on six biological replicates.

Transcriptomic analysis

Transcriptomic raw data obtained by Doré *et al.* (2015, 2017) were re-analyzed in the present study with a particular focus on Pi transporters. Briefly, transcript levels were quantified by RNA-Seq in free-living mycelia (FLM), in mycelia growing on the root surface for 2 or 4 d and in ectomycorrhizas obtained on modified Melin-Norkrans medium (Doré *et al.*, 2015). To study the expression of genes in pre-infectious mycelia, that is before symbiotic structure differentiation, transcripts were quantified in FLM and in mycelia poured on the surface of *P. pinaster* seedlings both grown on modified Melin-Norkrans medium (Doré *et al.*, 2017). Transcript abundance was expressed as reads per kilobase million (RPKM). Gene regulation was expressed as fold change (RPKM in mycelium in contact with roots or from ectomycorrhizas/RPKM in FLM).

Statistical analyses

Data are presented as the mean of three (X-ray fluorescence maps and transcriptomic analyses) to seven replicates. Differences between means were analyzed by one-way ANOVA followed by Tukey honest significant difference (HSD) *post-hoc* tests. Data normality was checked using the Wilk-Shapiro test and, if necessary, the data were either square root or $\log_{10}$ transformed before the analysis. Values in percentage (fungal colonization rate and percentage ^{32}P) were transformed ($\arcsin\sqrt{x}$) as described by Legendre & Legendre (1998). All statistical analyses were performed with R software at the 5% level of statistical significance (R Development Core Team, 2004). Significant differences in transcript levels from transcriptomic analyses were identified according to Baggerly *et al.* (2003), as previously described (Doré *et al.*, 2017).

Results

Expression of *HcPT2* is strongly up-regulated by *P. pinaster*

The regulation of *HcPT1.1*, *HcPT1.2* and *HcPT2* expression in response to symbiotic establishment was investigated by comparing their transcript abundance in the transcriptomic data from Doré *et al.* (2017). As shown in Table 1, transcripts of all three genes were detected in free-living mycelia, in mycelia growing on the root surface for 2 or 4 d, and in ectomycorrhizas. The expression levels of *HcPT1.1* and *HcPT1.2* were unchanged in mycelia poured on the root surface for 2 or 4 d, and slightly up-regulated and down-regulated in ectomycorrhizas compared to free-living mycelia, respectively. Also, *HcPT1.2* expression was very low under all conditions. By contrast, *HcPT2* was the only gene positively regulated in mycelia growing at the root surface for 4 d, before symbiotic structure differentiation (fold-change > 4.7). It was also strongly up-regulated in ectomycorrhizas (fold-change > 9). We focused on *HcPT2* because its expression was (1) higher by an order of magnitude and (2) more highly induced in response to mycorrhizal formation than the other candidate genes.

HcPT2 proteins are localized at both uptake and release sites of ectomycorrhizas

To enable the *in situ* localization of HcPT2, GFP-fusions, immunolocalization and transmission electron microscopy were used on 2-month-old ectomycorrhizas. No fluorescence was detected in ectomycorrhizas produced with the fungus expressing the empty vector (Fig. S4). Using GFP-fusions, fluorescence was detected in all tissues of ectomycorrhizas formed by the two transgenic fungal isolates, PT2-EGFP-1 and PT2-EGFP-5 (Fig. S4). A similar pattern of protein localization was observed using HcPT2-specific antibodies coupled with fluorescent dyes (Fig. 1a). Therefore, these two independent strategies demonstrated that HcPT2 proteins were localized at both Pi uptake (extra-radical hyphae and fungal mantle) and release (Hartig net)

Table 1 Expression levels of the three *Hebeloma cylindrosporum* H^+:Pi symporter genes, *HcPT1.1*, *HcPT1.2* and *HcPT2*, in free-living mycelia (FLM), in mycelia growing on the root surface (+plant) or in ectomycorrhizas, after different time of contact between the two partners

Contact time	Biotrophic status	Transcript abundance (RPKM) of:		
		HcPT1.1	*HcPT1.2*	*HcPT2*
2 d	FLM	44.24	15 .85	223.41
	+ plant	72.5	7.62	339.51
	Fold change	1.6	−2.1	1.5
	P	NS	NS	NS
4 d	FLM	50.63	10.99	159.24
	+ plant	96.97	7.87	751.95
	Fold change	1.9	−1.4	4.7
	P	NS	NS	0.000
3 wk	FLM	32.93	7.82	44.87
	Ectomycorrhizas	75.15	3.24	415.22
	Fold change	2.3	−2.4	9.3
	P	0.042	0.045	0.0012

Transcript abundance is expressed as reads per kilobase million (RPKM). Gene induction level is expressed as fold-change (RPKM in + plant mycelia or ectomycorrhizas/RPKM in FLM) whose significance (*P*) is given by the Baggerly test (Baggerly *et al.*, 2003). NS: not significant at $P \leq 0.05$.

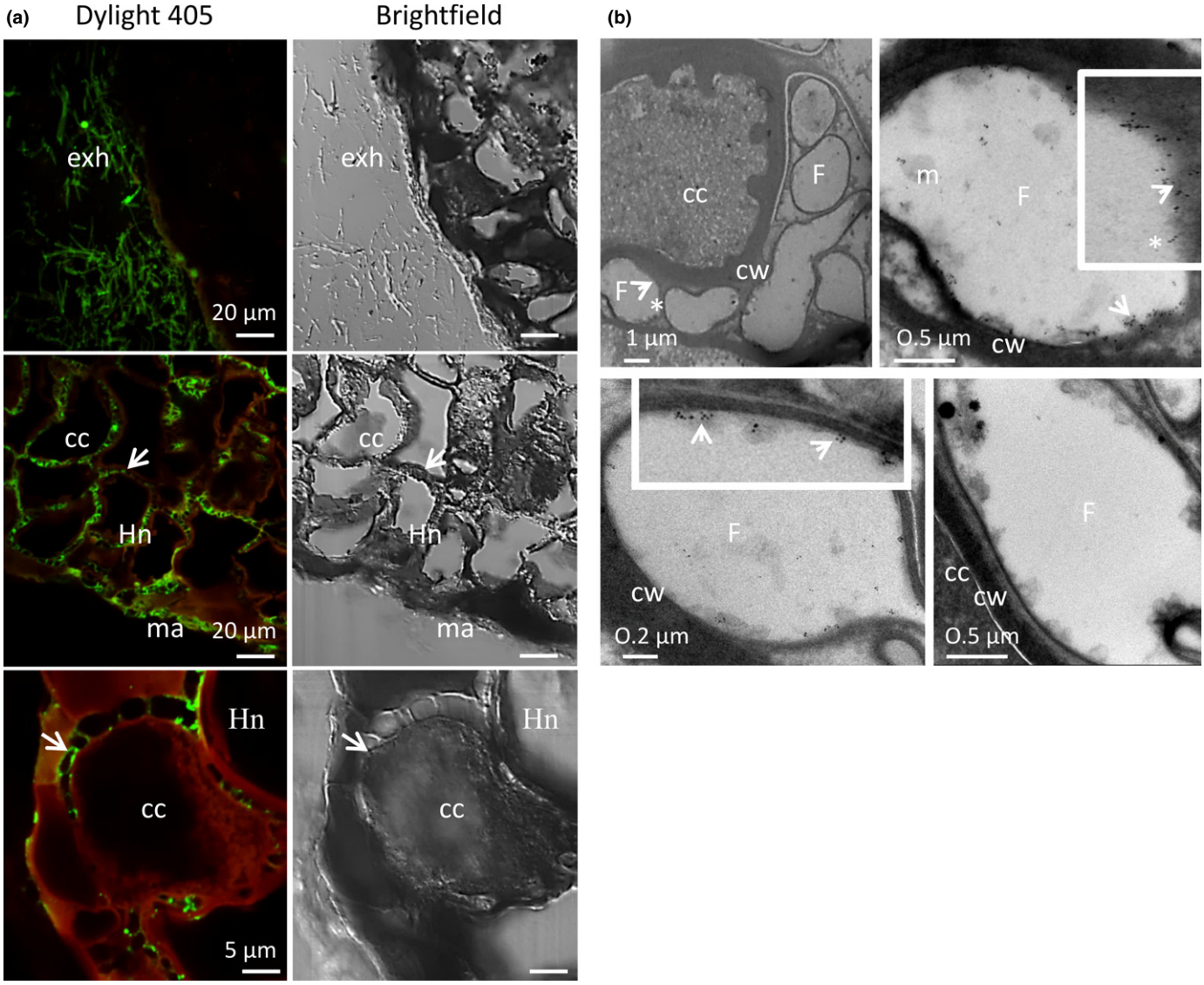

Fig. 1 Localization and sublocalization of the HcPT2 phosphate transporter. (a) Immunolocalization of HcPT2 in colonized roots. Laser scanning confocal microscopy images of ectomycorrhizal (ECM) roots were probed with HcPT2 antibodies and visualized with a secondary antibody conjugated with Dylight 405 (false color in green) on 7-µm cross-sections. Cell wall autofluorescence was acquired in red. (b) Immunogold-TEM localization of HcPT2. Using the anti-PT2, labeling was observed in the Hartig net. Arrows point to HcPT2-associated gold granules localized at the plasma membrane of fungal cells. At the right bottom, a control section is shown without the primary antibody. cc, cortical cell; cw, plant cell wall; exh, extra-radical hyphae; F, fungal cell; Hn, Hartig net; ma, hyphal mantle; m, mitochondria.

sites of ectomycorrhizas. To determine the subcellular localization of HcPT2 proteins in the fungal hyphae forming the Hartig net, we used transmission electron microscopy coupled with immunogold labeling (Fig. 1b). No labeling was detected without primary antibodies. By using primary antibodies targeting the intracellular part of HcPT2, we observed gold granules predominantly along the plasma membrane of fungal cells (Fig. 1b).

Modification of *HcPT2* expression impacts fungal growth and ectomycorrhiza formation

To further dissect the role of HcPT2 in Pi acquisition during symbiosis, transgenic fungal lines down- or up-regulating *HcPT2* were produced and analyzed. The expression of *HcPT2* in silencing lines decreased by 27% (RNAi-PT2-6) and 52% (RNAi-PT2-9), and increased in both overexpressing isolates (OE-PT2-4 and OE-PT2-7) to *c.* 400% compared to the control (Ctl) (Fig. 2a). In these transgenic fungal lines with modified *HcPT2* expression, the expression of the two other H^+:Pi symporters, *HcPT1.1* and *HcPT1.2*, was not altered (Fig. S5a,b). Despite the different levels of *HcPT2* expression, the growth of transgenic mycelia was not affected (both overexpressing lines and RNAi-PT2-6) or decreased slightly (*c.* 30%, RNAi-PT2-9) compared to Ctl (Fig. 2b).

We assessed the capacity of these transgenic lines to form ectomycorrhizas by co-culturing them with *P. pinaster* either in solid nutrient medium or in soil, using the wild-type and Ctl strains as control. After 4 wk on solid medium, the morphology and

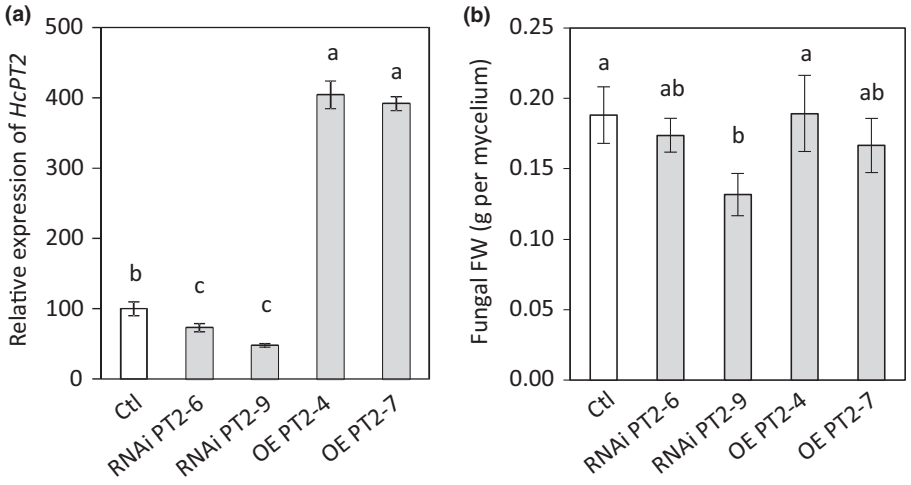

Fig. 2 Characterization of *HcPT2* transgenic lines of *Hebeloma cylindrosporum* transformed with the empty vector (Ctl), the RNAi construct (RNAi-PT2-6 and RNAi-PT2-9) and the overexpression construct (OE-PT2-4 and OE-PT2-7) grown in pure culture. (a) Relative expression of *HcPT2* quantified using quantitative reverse transcriptase PCR and normalized using the α-tubulin housekeeping gene from *H. cylindrosporum*. (b) Biomass of the fungi grown in the same culture conditions. Bars correspond to mean values ± SD ($n = 6$). Different letters indicate significant differences between the fungal lines according to one-way ANOVA followed by Tukey's HSD test at $P < 0.05$.

number of ectomycorrhizas per plant were similar between both control strains and the overexpressing ones, *c.* 20 ectomycorrhizas per plant (Table 2; Fig. S6). This indicates that the overexpression of *HcPT2* did not modify the capacity of the fungus to form ectomycorrhizas. By contrast, both RNAi-PT2-6 and RNAi-PT2-9 lines developed significantly less ectomycorrhizas, 10 and five per plant, respectively, and no external mycelium was observed (Table 2; Fig. S6). Therefore, the down-regulation of *HcPT2* strongly altered the ability of the fungus to grow on plant roots and ultimately to form mature ectomycorrhizas.

These observations were confirmed when *P. pinaster* was co-cultured with the control and transgenic fungal strains in soil under high and low P regimes (Fig. 3). Growth on plant roots of lines down-regulating *HcPT2* expression was drastically affected (Fig. 3a). Quantitative image analysis showed that the control strains (h7 and Ctl) and the overexpressing isolates similarly displayed *c.* 2.4% of relative fungal growth area in both +P and −P conditions (Fig. 3b). By contrast, hyphal growth was significantly reduced in the two RNAi lines compared to the controls, especially in −P soil where no fungal growth was observed on roots.

Table 2 Ectomycorrhizal (ECM) root tip formation between wild-type or transgenic strains of *Hebeloma cylindrosporum* and *Pinus pinaster*

Fungal strain	ECM root tips (number per plant)
NM	0c
h7	21.0 ± 5.7a
Ctl	19.4 ± 5.2a
RNAi-PT2-6	10.3 ± 4.1b
RNAi-PT2-9	5.6 ± 3.3bc
OE-PT2-4	22.6 ± 3.5a
OE-PT2-7	19.4 ± 5.2a

The number of ECM root tips per plant was determined after 4 wk of co-culture. The number of ectomycorrhizas using RNAi-PT2 strains was significantly reduced in comparison to wild-type and Ctl strains. The corresponding photographs are presented in Supporting Information Fig. S6. Data are given as means ± SD ($n = 7$). Different letters indicate significant differences between the fungal lines according to one-way ANOVA followed by Tukey's HSD test at $P < 0.05$.

In +P soil, only 0.8% of relative fungal growth area was observed for RNAi-PT2-6 and 0.1% for RNAi-PT2-9.

Modification of *HcPT2* expression affects the phosphorus status of mycorrhizal *P. pinaster*

The effects of the transgenic lines on P accumulation in plants grown in soil conditions were quantified. Total P contents in roots and shoots of plants colonized by the Ctl and wild-type fungal strains were similar (Fig. S7), enabling the use of Ctl as the sole control treatment in further experiments. Plants co-cultivated with the control fungus accumulated more P in roots and shoots than NM plants (Figs 4, S7). In +P soil, only plants colonized by RNAi-PT2-9 displayed a reduction of P in shoots and roots, compared to the control fungus, reaching a similar amount to NM plants (Fig. 4a). However, plants colonized by both OE-PT2-4 and OE-PT2-7 isolates displayed a significant increase of P accumulation in shoots and roots compared to the plants inoculated with the control line (Fig. 4a).

In −P soil, plants colonized by the RNAi fungal lines accumulated less total P in roots and shoots than those inoculated by the control line, comparable to NM plants (Fig. 4b). This result was certainly due to the absence of ectomycorrhizas observed with RNAi lines (Fig. 3). Higher shoot P contents were measured in plants colonized by both OE-PT2 fungal lines compared to those inoculated with the control, despite similar root P contents (Fig. 4b). This enhanced P accumulation in shoots can be attributed mainly to the overexpression of *HcPT2* in the fungus as no difference in ECM colonization was observed for all these plants (Fig. 3).

Overexpression of *HcPT2* increases phosphorus levels in the central cylinder and in the cortical cells of ectomycorrhizal roots

To get a more precise pattern of *in planta* P concentrations due to the overexpression of *HcPT2*, the P distribution in ectomycorrhizas was mapped using Synchrotron X-ray fluorescence. Roots were associated with the control (Ctl) or OE-PT2-4 fungal

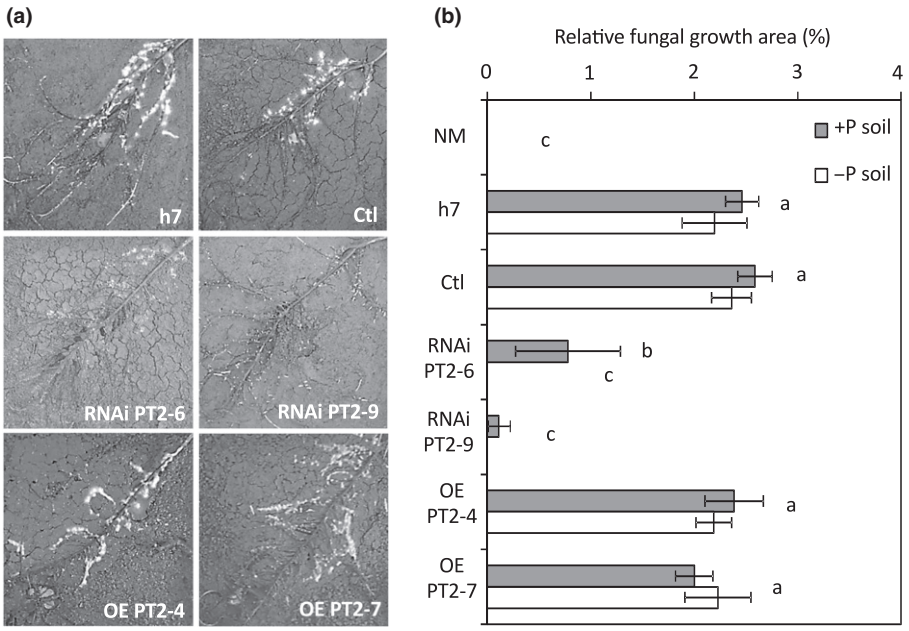

Fig. 3 Relative growth of wild-type and transgenic *Hebeloma cylindrosporum* strains on *Pinus pinaster* roots. (a) Pictures of *P. pinaster* roots associated with the wild-type (h7), empty vector (Ctl), *HcPT2*-silencing (RNAi-PT2-6 and RNAi-PT2-9) or *HcPT2*-overexpressing (OE-PT2-4 and OE-PT2-7) fungal strains. (b) The relative fungal growth was analyzed using IMAGE J software on 70-d-old plants grown under inorganic phosphate (Pi)-sufficient (+P soil) and Pi-deficient (−P soil) conditions. Bars correspond to mean values ± SD ($n = 6$). Different letters indicate significant differences between the fungal lines according to one-way ANOVA followed by Tukey's HSD test at $P < 0.05$.

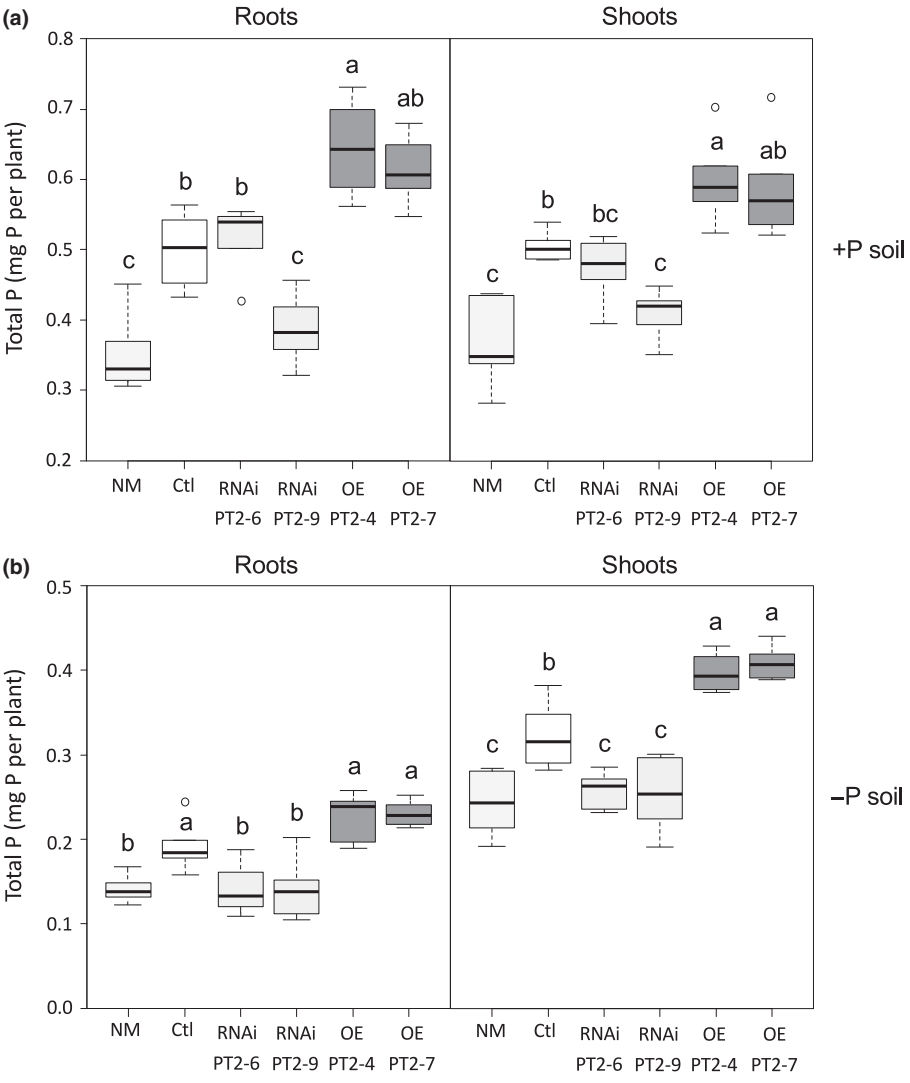

Fig. 4 Total phosphorus (P) accumulation in *Pinus pinaster* plants associated with *Hebeloma cylindrosporum* transgenic lines affected in *HcPT2* expression. Total P was measured in roots and shoots of nonmycorrhizal plants (NM) and plants inoculated with the fungal strain harboring the empty vector (Ctl), or the silencing (RNAi-PT2-6 and RNAi-PT2-9) or overexpressing (OE-PT2-4 and OE-PT2-7) constructs during 70 d under inorganic phosphate (Pi)-sufficient (a) and Pi-deficient (b) conditions. Box-plots indicate the median, the 1st and 3rd quartiles, and bars give the smallest and highest values of observations ($n = 6$); empty circles indicate outliers. Different letters indicate significant differences between the fungal lines according to one-way ANOVA followed by Tukey's HSD test at $P < 0.05$.

strains or kept noncolonized (NM). The heat map showed that nuclei always displayed the highest P fluorescence in NM and control sections (Fig. 5a). In OE-PT2-4 sections, some areas corresponding to the central cylinder displayed similar P fluorescence levels to the nuclei, indicating that these tissues accumulated more P when the overexpressing line colonized the plant. Levels of P X-ray fluorescence signal, which are directly proportional to P concentrations, were greatest in the central cylinder the lowest in the vacuoles of cortical cells, whatever the root type (Fig. 5b). Compared to NM roots, the control fungal strain increased P concentrations 3.5-fold in the central cylinder, 2.6-fold in the cytosol and 2.1-fold in the vacuoles of the cortical cells. OE-PT2-4 led to greater increases of P fluorescence compared to NM roots, by 6.8-fold in the central cylinder, 8.7-fold in the cytosol and 6.4-fold in the vacuoles of the cortical cells. Relative to the control line, fluorescence intensity was increased three-fold in root sections colonized by OE-PT2-4 fungal strains, confirming that an increase of *HcPT2* expression resulted in an increase of P in all cellular compartments from the host plant.

HcPT2 expression levels modify the uptake and unloading of ^{32}Pi from *H. cylindrosporum* mycelia towards *P. pinaster* roots

We previously showed that *H. cylindrosporum* mycelia released greater amounts of ^{32}P when incubated with *P. pinaster* (Torres-Aquino *et al.*, 2017). Using the same experimental design, we examined how *HcPT2* expression levels affect both ^{32}P uptake and release capacities by the fungal transgenic lines. Compared to Ctl mycelia, *HcPT2* down-regulation reduced hyphal growth and strongly impaired the amount of ^{32}Pi taken up by the fungus during the 16 h period (Fig. S8a–b). These results indicate that HcPT2 mediated an important fraction of Pi uptake under these conditions. Only OE-PT2-4 displayed a significant increase in biomass and ^{32}P accumulation compared to the Ctl fungal strain (Fig. S8a–b). However, the two overexpressing lines displayed similar Pi uptake as the Ctl line when normalized per gram of fresh weight (Fig. 6a). This indicates that the up-regulation of *HcPT2* did not improve Pi acquisition capacity of the fungus under these conditions.

^{32}P-labeled mycelia were also incubated with or without pine seedlings for 48 h in an induction medium free of P and carbon. Without the plants, all fungal strains released a similar amount of ^{32}P (Fig. S9). The Ctl and the two RNAi lines released comparable amounts of ^{32}P in the medium, regardless of plant presence. By contrast, the two overexpressing strains released more ^{32}P in the interaction medium compared to the Ctl and RNAi lines. This release was enhanced four- and 13-fold in the presence of the plant for OE-PT2-4 and OE-PT2-7, respectively (Fig. S9). Also, the amount of ^{32}P detected in the plants incubated with the Ctl and overexpressing lines was respectively 7.5- (Ctl), 11- (OE-PT2-4) and 10.5- (OE-PT2-7) fold higher than in plants incubated with RNAi-PT2-6 and RNAi-PT2-9 (Fig. S9).

The low amount of ^{32}P released by the RNAi strains could be due to their low ^{32}Pi uptake capacity. Therefore, to normalize the fungal ^{32}Pi uptake for all strains, we also expressed the results as the percentage of total ^{32}P accumulated in the fungi at the beginning of the experiment. Without plants, both RNAi strains

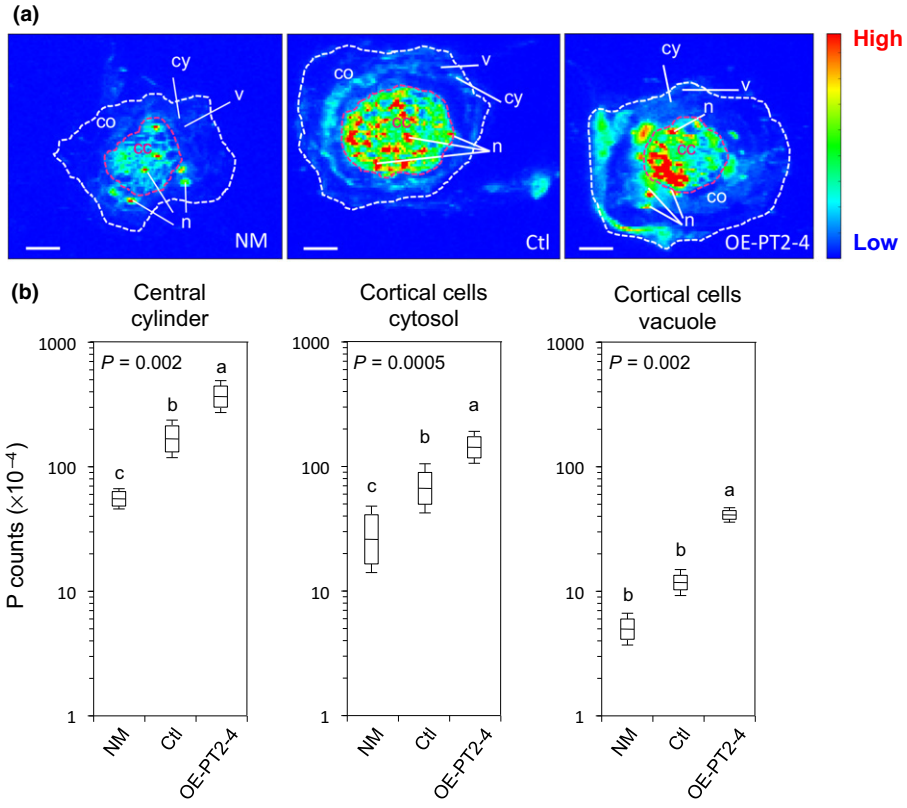

Fig. 5 Phosphorus (P) distribution in *Pinus pinaster* short roots colonized by *Hebeloma cylindrosporum* transgenic lines either expressing the empty vector (Ctl) or overexpressing *HcPT2* (OE-PT2-4), or kept noninoculated (NM). (a) X-ray fluorescence maps showing the intensity of elemental P in 20 μm cross-sections (bars, 50 μm). (b) P counts from the pixels extracted from different root and cell compartments (see details in Supporting Information Methods S1). Box-plots indicate the mean, with the standard error and standard deviation of the mean ($n = 3$). Statistical differences between means were calculated with one way-ANOVA and different letters indicate significant differences between root types. cc, central cylinder; co, cortex; cy, cytosol; n, nuclei; v, vacuole. The white dashed line indicates the limits of the root cortex, also containing the fungal mantle in the ectomycorrhizal (ECM) sections. The pink dashed line indicates the external limit of the central cylinder ($n = 3$).

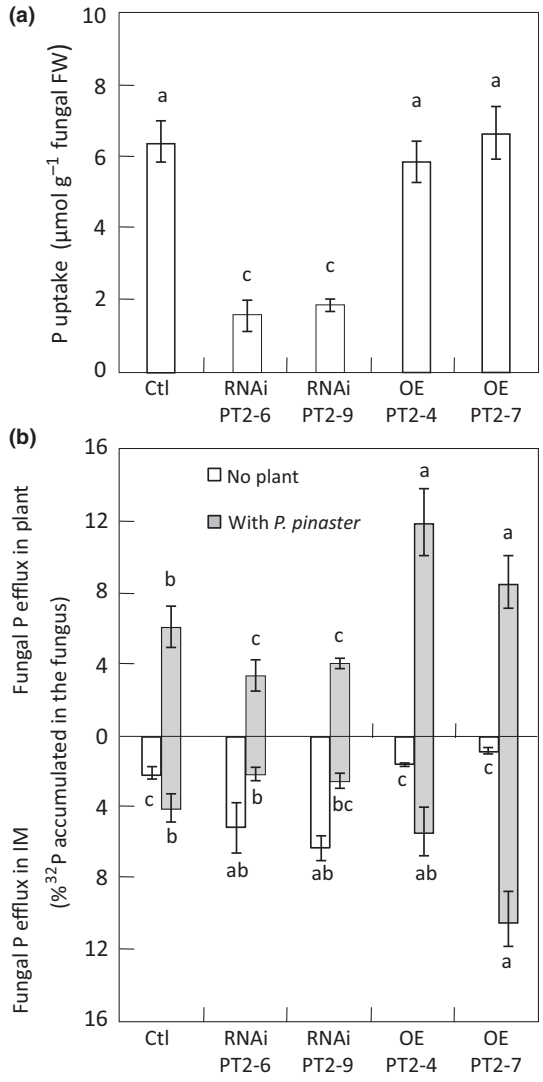

Fig. 6 ^{32}P uptake and release by *Hebeloma cylindrosporum* mycelia harboring the empty vector (Ctl), or the HcPT2-silencing (RNAi-PT2-6 and RNAi-PT2-9) or overexpressing (OE-PT2-4 and OE-PT2-7) construct. (a) Phosphorus (P) uptake during the ^{32}Pi loading period (16 h), expressed in micromoles of inorganic phosphate (Pi) per gram of fungal fresh weight. (b) ^{32}P release from *H. cylindrosporum* transgenic lines, accumulated in plants (upper panel) or in the interaction medium (IM, lower panel). In (b), *H. cylindrosporum* mycelia were incubated alone (white bars) or with *P. pinaster* roots (grey bars) over 48 h. The amounts of total ^{32}P released in the plant and in the interaction medium were expressed as a percentage of the total ^{32}P present in the fungi at the beginning of the experiment according to the values in Fig. S8(b). Values are the means ± SE ($n = 6$). Different letters indicate significant differences between means of ^{32}P fluxes into the interaction medium and the plants using one-way ANOVA followed by Tukey's HSD test at $P < 0.05$.

released more ^{32}P (*c.* 6%) than the Ctl and the OE strains (*c.* 2%) into the interaction medium (Table 3; Fig. 6b). However, with or without plants, RNAi lines released a similar percentage of ^{32}P (*c.* 6%) (Table 3). When incubated with RNAi strains, plants accumulated *c.* 3.5% of ^{32}P released, a percentage significantly lower than when incubated with the Ctl and both overexpressing lines (Fig. 6b). By contrast, Ctl, OE-PT2-4 and OE-PT2-7 strains have lost more ^{32}P when incubated with than without plants (Table 3). Thus, the total release of accumulated ^{32}P (interaction medium + plants) was much greater from the overexpressing strains (≥ 17%) than the RNAi strains (Table 3). Similarly, plants incubated with the overexpressing strains acquired more ^{32}P, previously taken up and released by the fungi, than those incubated with the Ctl strain (Fig. 6b).

Discussion

The H^+:Pi symporter HcPT2 of *H. cylindrosporum* was previously found to be highly expressed in ectomycorrhizas under both high and low P availability (Tatry *et al.*, 2009), suggesting a role in symbiotic Pi transport. Complementary to this, the most salient results recorded in the present work showed that HcPT2 is essential not only for both Pi acquisition by extramatrical hyphae and release toward host plant, but also for differentiation of symbiotic structures.

HcPT2 is essential for the differentiation of symbiotic structures and the Pi nutrition of ectomycorrhizal plants

HcPT2 was expressed in free-living hyphae and up-regulated in the pre-infectious mycelia (in the presence of the host root, before symbiotic structure differentiation) as well as in ectomycorrhizas (Doré *et al.*, 2017). This suggests a role in both fungal vegetative growth and the establishment and functioning of symbiotic structures. We further investigated this hypothesis by studying the mycorrhizal activity of transgenic lines affected in *HcPT2* expression. Interestingly, RNAi strains under-expressing *HcPT2* were greatly impaired in their ability to colonize *P. pinaster* roots, suggesting a key role for HcPT2 in both the development of extra-radical hyphae and the formation of functional ectomycorrhizas. As this phenotype was drastic when Pi availability was limited, we assume that HcPT2 plays a unique role that cannot be compensated for by other Pi transporters. Interestingly, the artificial down-regulation of the high-affinity H^+:Pi symporter *GigmPT* of the arbuscular mycorrhizal species *Gigaspora margarita* also resulted in impaired symbiotic structures in *Astragalus sinicus* roots (Xie *et al.*, 2016). The authors proposed that the disruption of *GigmPT* affected signal(s) coordinating arbuscule differentiation. Whether HcPT2 and GigmPT act via a 'simple' nutritional effect or are component(s) of signaling network(s) essential for mycorrhizal symbiosis establishment remains to be elucidated.

It is noteworthy that *P. pinaster* plants associated with transgenic lines overexpressing *HcPT2* accumulated more P in their shoots than those associated with the corresponding control strain. This indicates that, besides being essential for fungal growth and symbiotic structure differentiation, HcPT2 was also a key component of the beneficial effect of the fungal partner on host plant Pi nutrition. By mapping P levels in pine root tissues, we showed that ECM association with a control fungus improved P content in both root cortex and central cylinder. This effect was enhanced in plants colonized by the fungal strains overexpressing *HcPT2*, reinforcing the view of HcPT2 playing an essential role in Pi delivery to host roots. In this context, it was

Incubation	Total ^{32}P (% of initial ^{32}P in the fungus) released by:				
	Ctl	RNAi-PT2-6	RNAi-PT2-9	OE-PT2-4	OE-PT2-7
No plant	2.5 ± 0.3c	5.1 ± 1.3b	6.2 ± 0.7b	1.9 ± 0.2c	1.5 ± 0.2c
With *P. pinaster*	10.5 ± 1.3ab	5.8 ± 0.9b	6.9 ± 0.8b	17.0 ± 2.0a	18.7 ± 1.9a

Values are expressed as percentage of the total ^{32}P present in the fungi at the beginning of the experiment according to the values in Fig. S8(b). Data are means ± SE ($n = 6$). Different letters indicate significant differences between the culture conditions according to one-way ANOVA followed by Tukey's HSD test at $P < 0.05$.

Table 3 Total amounts of ^{32}P (measured in interaction medium and plants) released by the *Hebeloma cylindrosporum* transgenic fungal strains (Ctl, RNAi-PT2-6, RNAi-PT2-9, OE-PT2-4 and OE-PT2-7) during the symbiotic interface-mimicking experiment, when incubated alone (no plant) or with plant roots (with *Pinus pinaster*)

tempting to speculate that HcPT2 is involved in Pi efflux from fungal hyphae in the Hartig net.

HcPT2 expression impacts both acquisition and release of Pi under control of the host plant

RNAi transformants down-regulating *HcPT2* accumulated less ^{32}P in free-living mycelia than the overexpressing and control lines when P was resupplied to P-starved mycelia. This further substantiated our hypothesis that HcPT2 is involved in Pi uptake from the external medium; this is a role that it may play in hyphae not in contact with host roots, that is in free-living mycelium or extra-radical hyphae of ECM plants (Fig. 7a). Such a role in Pi uptake has already been ascribed to HcPT2 (Tatry *et al.*, 2009) as well as for other H^+:Pi symporters whose proteins or transcripts were detected in ECM (Garcia *et al.*, 2013; Wang *et al.*, 2014; Zheng *et al.*, 2016) or arbuscular mycorrhizal (AM) (Harrison & van Buuren, 1995; Xie *et al.*, 2016) fungi. The fact that transgenic lines overexpressing *HcPT2* were unaffected in their Pi uptake could be due to a saturation of the Pi transport in nonlimiting Pi concentrations. We can also hypothesize that other mechanism(s) related to P assimilation such as polyP synthesis, could act as limiting factor(s) for supplementary Pi uptake.

When incubated in the interaction medium without *P. pinaster* roots, down-regulating *HcPT2* mycelia released a greater proportion of ^{32}P than overexpressing and control lines. These results suggest that another mechanism and/or P transporter than HcPT2 could mediate the release of ^{32}P in *HcPT2* down-regulating lines. Simultaneously, ^{32}P exported by an HcPT2-independent mechanism could be less re-imported by *HcPT2* down-regulating lines and more re-imported by *HcPT2* over-expressing lines, supporting a role of HcPT2 as a Pi importer under these conditions (free-living mycelium).

The situation was different with hyphae in contact with host roots. Indeed, RNAi lines were impaired in ^{32}Pi unloading into the interaction medium, whereas strains overexpressing *HcPT2* released more ^{32}P. Assuming that our experimental system mimics the interfacial apoplast of the Hartig net, data suggest a possible role for HcPT2 in Pi import into the mycelium and in its release at Hartig net hyphae under the influence of *P. pinaster* roots (Fig. 7b). Thus, HcPT2 could have a dual function, acting as both an influx carrier in extra-radical hyphae escaping plant control and an efflux carrier in intra-radical hyphae colonizing the root cortex.

This dual function would imply that HcPT2 transport of Pi in both directions through the plasma membrane. Interestingly, such a property was demonstrated for Pho84 shown to mediate P import into tightly sealed vesicles obtained from reverted yeast plasma membranes (Fristedt *et al.*, 1996). These data suggest that direction of P transport catalyzed by a high-affinity H^+:Pi symporter could occur in both directions through the plasma membrane, depending on the driving force and independently of the protein orientation. To date, heterologous expression of H^+:Pi transporters from mycorrhizal fungi in yeast has only been shown to have a role in Pi influx (Harrison & van Buuren, 1995; Tatry

Fig. 7 Schematic model showing the potential role of HcPT2 in the ectomycorrhizal (ECM) symbiosis as well as its hypothetical regulation and contribution to the global phosphorus (P) trafficking between symbiotic partners. (a) In extra-radical hyphae, inorganic phosphate (Pi) is taken up by HcPT2 (this study) and HcPT1.1 under limiting conditions (Garcia *et al.*, 2013). Other putative fungal transporter(s), such as the main candidates HcPho90 and HcPT1.2, might also contribute to Pi acquisition from the soil. In the cytosol, Pi is rapidly incorporated into the active pool of phosphate, including phosphorylated primary metabolites, structural molecules and nucleic acids, or transported into the vacuoles. In the vacuoles of extra-radical hyphae and fungal mantle, Pi is condensed into long-chain polyphosphates (polyPs) by (an) unknown enzyme(s), and translocated to the rest of the mycelium, including the intra-radical hyphae of the Hartig net (reviewed by Cairney, 2011). (b) In the Hartig net, long-chain polyPs are hydrolyzed into short-chain polyPs (reviewed by Cairney, 2011; Torres-Aquino *et al.*, 2017). Short-chain polyPs are then further hydrolyzed into free Pi, which is released into the cytosol by an unidentified transport system(s). In response to unidentified signals emanating from the host plant (dashed arrow), the free cytosolic Pi is released into the symbiotic interface. This export could be mediated by HcPT2 and would involve its post-transcriptional and/or post-translational modification to allow transport of Pi against pH gradients (yellow star). Because HcPT1.1 proteins were also detected in intra-radical hyphae (Garcia *et al.*, 2013), this transporter might also play a role at the symbiotic interface. Also, we cannot exclude the presence of other transporter(s) participating in the release of Pi from the fungus to the interface, including HcPho90, HcPHO1 and HcPT1.2. Similarly, although it has never been demonstrated in ECM fungi, an independent vesicle trafficking pathway transporting free Pi from the tonoplast to the plasma membrane might also coexist. Finally, the acquisition of free Pi by *Pinus pinaster* cortical cells from the symbiotic interface, contributing to the increase of P contents in plant tissues (this study), involved as yet unidentified transporters. c.cyl, central cylinder; cc, cortical cells; ec, epidermal cells; end, endoderm.

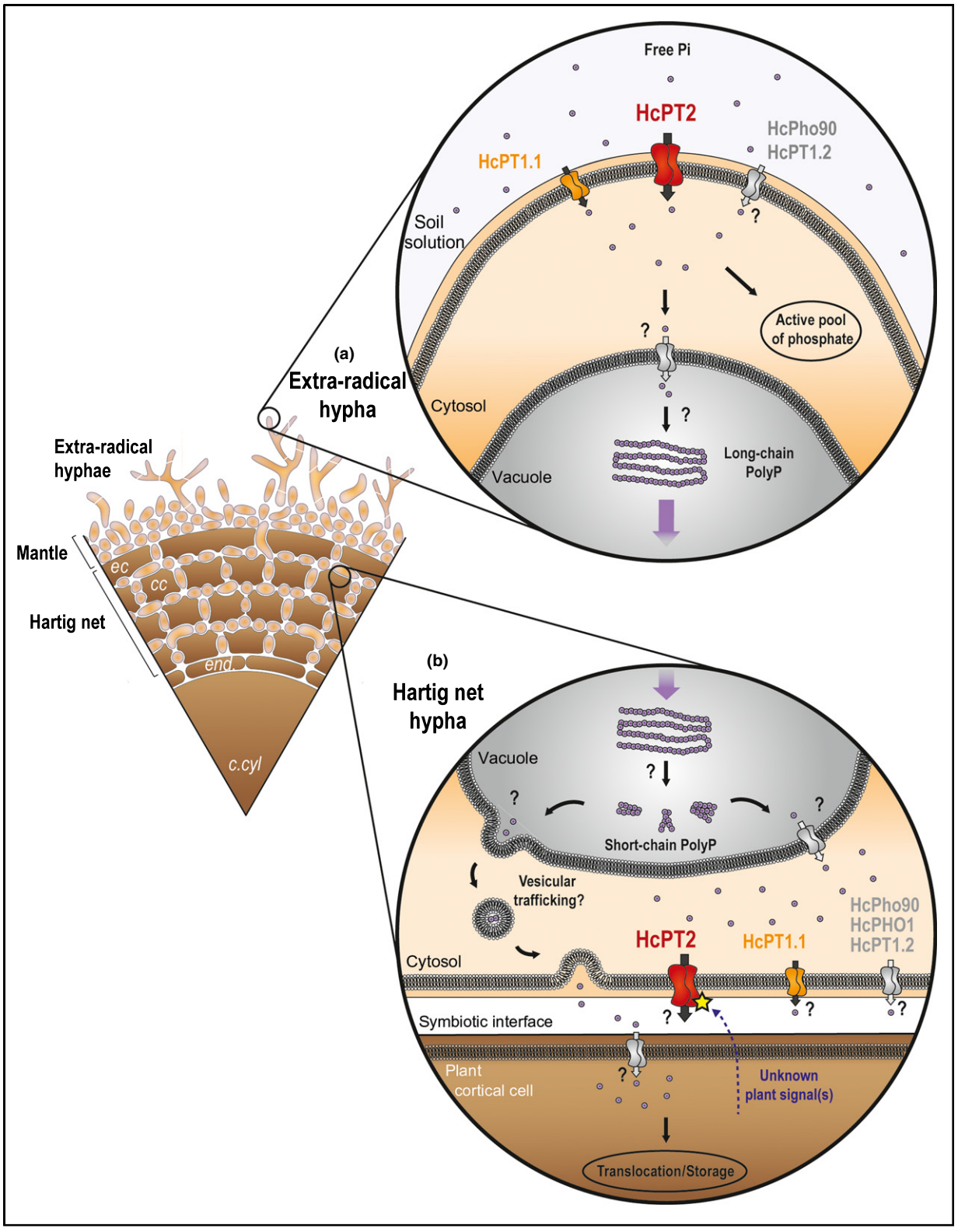

et al., 2009; Wang *et al.*, 2014; Xie *et al.*, 2016). As shown for plant H^+:Pi transporters, this could be due to methodological limitations (Guo *et al.*, 2008; Cubero *et al.*, 2009; Preuss *et al.*, 2010).

Identification of the mechanism(s) controlling the direction of Pi flux across HcPT2 will be of key importance to further elucidate its role in Pi trafficking from soil to the host plant. Recently, Schott *et al.* (2016) simulated *in silico* Pi and sugar exchanges in

AM symbiosis and proposed that fungal and plant H^+:Pi and H^+:sugar transport systems may work in a concerted manner. Proton-dependent Pi influx in plant cells and proton-dependent sugar influx in fungal cells allow in return proton-dependent Pi efflux from the fungal cells and proton-dependent sugar efflux from the plant cells, respectively. Based on these simulations, the authors demonstrated that Pi efflux occurred from fungal cells even at low apoplastic pH. However, ATPase activity and concentration gradients of Pi and sugar over the plasma membranes were decisive in the magnitude of export rates. In this respect, Torres-Aquino *et al.* (2017) demonstrated that *P. pinaster* induced the hydrolysis of *H. cylindrosporum* vacuolar polyPs in mycelia incubated in the Hartig net-mimicking system. Such polyP breakdown in the fungal cells in the Hartig net could increase Pi concentrations in the fungal vacuoles, and subsequently stimulate the export of Pi into the cytosol favoring Pi efflux (Fig. 7), even if the Pi concentration in the cytosol is tightly regulated (Wild *et al.*, 2016). This would not occur in the absence of the host plant, that is in free-living mycelia or in extraradical hyphae of mycorrhizal systems, which have a low cytosolic Pi concentration favorable for Pi influx (Fig. 7).

There is no reason to consider that such regulatory mechanisms would be specific to HcPT2. However, because we showed that *HcPT2* was the most transcribed Pi transporter-encoding gene in ectomycorrhizas (see Table 1), it can be reasonably assumed that *HcPT2* is the primary target of these regulatory mechanisms. Another possible explanation for the dual behavior of HcPT2 could be its conversion from an H^+:Pi symporter into a Pi uniporter under control of the host plant. Such conversion might be mediated by post-translational modification(s) of the proteins (e.g. phosphorylation) or by the allosteric interaction of HcPT2 with another phosphorylated protein, as demonstrated for the conversion of a lactose:H^+ symporter into a sugar uniporter in bacteria (Ye *et al.*, 1994). However, further experiments are needed to unravel the regulation mechanism(s) of HcPT2 in axenic vs symbiotic conditions.

While our data suggest that HcPT2 could participate in Pi export from fungal cells, other candidates might also play this role (Nehls & Plassard, 2018). Besides HcPT1.1 and HcPT1.2, other not yet characterized fungal Pi transporter(s) could also participate in Pi allocation to the host roots. Indeed, the transporters ScPho90 and AtPHO1 were shown to be responsible for Pi efflux in yeast (Hürlimann *et al.*, 2009) and *Arabidopsis thaliana* (Arpat *et al.*, 2012, Wege *et al.*, 2016), respectively. A BlastP search against the protein database of *H. cylindrosporum* (https://genome.jgi.doe.gov/Hebcy2/Hebcy2.home.html) resulted in the identification of a protein (ID #447161) that displayed 71.3% similarity with ScPho90 and was named HcPho90. Another protein (ID #440607), named HcPHO1, showed 67.6-% similarity to AtPHO1. HcPho90 is not an ideal candidate for a role in Hartig net Pi efflux because it was not significantly up-regulated in ectomycorrhizas (data not shown). HcPHO1 could be a better candidate as it was up-regulated 5.6-fold in ectomycorrhizas. However, its expression level in ectomycorrhizas was 8.3 times lower than that of HcPT2 (50.19 vs 415.22 RPKM). Nevertheless, in the absence of further results, the involvement of HcPho90 and HcPHO1 in Pi efflux from the Hartig net cannot be ruled out (Fig. 7b). Finally, although no evidence is currently available, a vesicular trafficking pathway from the vacuoles of the Hartig net hyphae towards the plasma membrane, without the involvement of transporters, cannot be excluded for the release of Pi into the apoplast (Fig. 7b).

HcPT2 is up-regulated by unknown diffusible signal(s) of plant origin

Besides being up-regulated in ectomycorrhizas as compared to free-living mycelia, *HcPT2* expression was also found to be induced after a 4 d contact with *P. pinaster*, that is before adhesion to the root and before symbiotic structure differentiation. This early induction is in line with our previous conclusion that HcPT2 is essential for symbiotic structure differentiation and suggests that the modulation of *HcPT2* expression is a component of the molecular cross-talk acting upstream of symbiosis establishment. This view also emphasizes the importance of nutrients as signals themselves in the establishment of the ECM symbiosis (Garcia *et al.*, 2015). Because this up-regulation took place upon early contact with the root, in the absence of symbiotic structure, it can reasonably be assumed that it was induced by (a) diffusible molecule(s) released by the plant and perceived by a compatible fungus. So far, the chemical nature of the signal remains elusive. It could be small molecules such as ethylene, auxin, or flavonoids generally produced during the interaction between fungi and plants (Plett *et al.*, 2017). They could trigger *HcPT2* up-regulation via regulatory cascade(s), which remain to be elucidated. In this respect, Plett *et al.* (2017) demonstrated that *Populus trichocarpa* is able to release a subset of small secreted proteins that can enter hyphae of the ECM partner *Laccaria bicolor*, move toward the fungal nucleus, and finally affect the expression of fungal genes. A similar cross-talk might be responsible of the *P. pinaster*-induced *HcPT2* up-regulation. As mimicked by RNAi transformants down-regulating *HcPT2* that were impaired in their mycorrhizal ability, the failure of this dialogue, for example in the presence of an incompatible host plant, would result in the abortion of the symbiotic relationship.

Future challenges will be the identification of upstream regulatory network(s) regulating *HcPT2* transcription in symbiotic structures and the detection of eventual post-translational protein maturation or protein–protein interactions, which might affect the bidirectional functioning of this transporter.

Acknowledgements

The authors are grateful to the three anonymous reviewers and the editor for their constructive comments and suggestions that greatly helped us to improve the manuscript. This work was supported by the ANR project 'TRANSMUT' 2010 BLAN 1604 03 and by the program 'Investments for the future' (ANR-10-LABX-04-01) through the use of the Ecotrop platform from CeMEB labEx. We thank Alejandro Pardo and Minna J. Kemppainen from Universidad Nacional de Quilmes (Argentina) for

kindly supplying the plasmid pSILBAγ used for construction of the RNAi silencing vector. We acknowledge SOLEIL for provision of their synchrotron radiation facilities (proposal 20160232) and we would like to thank all the LUCIA beamline staff for assistance in using the beamline, together with Nicolas Leclercq for the development and support of the FLYSCAN data acquisition software. The authors are also grateful to Chantal Cazevieille for her technical assistance in TEM observation. They are also grateful to Dr Benoît Lacombe and Sandrine Negro for their help in ^{32}P measurements. We also thank Brandon Monier for critical proofreading of the manuscript. A.B. was supported by a fellowship from INRA (France) through a Contract for Young Scientist (CJS), and K.G. by grants from the French Minister of Research and Technology and the United States Department of Agriculture (USDA NIFA 2017-67014-26530). Microscopy observations were made at the Montpellier Rio Imaging facility (http://www.mri.cnrs.fr/).

Author contributions

A.B. performed most of the experiments with the help of L.A., S.R. and Y.B.; A.B. wrote the article with the contribution of K.G., S.D.Z., G.G. and C.P.; K.G. and A.B. produced the RNAi and the OE transgenic fungal lines, respectively; J.D. and G.G. produced and analyzed the RNA-seq data and W.S. contributed to western-blot analysis; C.P., C.R., L.A and C.T-S. performed the experiment at SOLEIL Synchrotron on the LUCIA beamline and B.L-K. supervised the experiment. C.P. and S.D.Z. conceived the project and supervised the experiments.

References

Ali MA, Louche J, Legname E, Duchemin M, Plassard C. 2009. *Pinus pinaster* seedlings and their fungal symbionts show high plasticity in phosphorus acquisition in acidic soils. *Tree Physiology* **29**: 1587–1597.

Arpat AB, Magliano P, Wege S, Rouached H, Stefanovic A, Poirier Y. 2012. Functional expression of PHO1 to the Golgi and trans-Golgi network and its role in export of inorganic phosphate. *Plant Journal* **71**: 479–491.

Ashford AE, Allaway WG. 2002. The role of the motile tubular vacuole system in mycorrhizal fungi. *Plant and Soil* **244**: 177–187.

Ashford AE, Ryde S, Barrow KD. 1994. Demonstration of a short chain polyphosphate in *Pisolithus tinctorius* and the implications for phosphorus transport. *New Phytologist* **126**: 239–247.

Ashford AE, Vesk PA, Orlovich DA, Markovina AL, Allaway WG. 1999. Dispersed polyphosphate in fungal vacuoles in *Eucalyptus pilularis*/*Pisolithus tinctorius* ectomycorrhizas. *Fungal Genetics and Biology* **28**: 21–33.

Baggerly KA, Deng L, Morris JS, Aldaz CM. 2003. Differential expression in SAGE: accounting for normal between-library variation. *Bioinformatics* **19**: 1477–1483.

Becquer A, Torres-Aquino M, Le Guernevé C, Amenc LK, Trives-Segura C, Staunton S, Quiquampoix H, Plassard C. 2017. A method for radioactive labelling of *Hebeloma cylindrosporum* to study plant–fungus interactions. *Bio-Protocol* **7**: e2576.

Becquer A, Trap J, Irshad U, Ali MA, Plassard C. 2014. From soil to plant, the journey of P through trophic relationships and ectomycorrhizal association. *Frontiers in Plant Science* **5**: 548.

Bun-ya N, Nishimura M, Harashima S, Oshima Y. 1991. The PHO84 gene of *Saccharomyces cerevisiae* encodes an inorganic phosphate transporter. *Molecular and Cellular Biology* **11**: 3229–3238.

Cairney JWG. 2011. Ectomycorrhizal fungi: the symbiotic route to the root for phosphorus in forest soils. *Plant and Soil* **344**: 51–71.

Casarin V, Plassard C, Hinsinger P, Arvieu J-C. 2004. Quantification of ectomycorrhizal fungal effects on the bioavailability and mobilization of soil P in the rhizosphere of *Pinus pinaster*. *New Phytologist* **163**: 177–185.

Casieri L, Lahmidi NA, Doidy J, Veneault-Fourrey C, Migeon A, Bonneau L, Courty P-E, Garcia K, Charbonnier M, Delteil A *et al.* 2013. Biotrophic transportome in mutualistic plant–fungal interactions. *Mycorrhiza* **23**: 597–625.

Combier J-P, Melayah D, Raffier C, Gay G, Marmeisse R. 2003. *Agrobacterium tumefaciens*-mediated transformation as a tool for insertional mutagenesis in the symbiotic ectomycorrhizal fungus *Hebeloma cylindrosporum*. *FEMS Microbiology Letters* **220**: 141–148.

Combier JP, Melayah D, Raffier C, Pepin R, Marmeisse R, Gay G. 2004. Nonmycorrhizal (Myc(-)) mutants of *Hebeloma cylindrosporum* obtained through insertional mutagenesis. *Molecular Plant–Microbe Interactions* **17**: 1029–1038.

Courty P-E, Doidy J, Garcia K, Wipf D, Zimmermann SD. 2016. The transportome of mycorrhizal systems. In: Martin F, ed. *Molecular mycorrhizal symbiosis*, 1st edn. Chichester, UK: John Wiley & Sons, 239–256.

Cubero B, Nakagawa Y, Jiang X-Y, Miura K-J, Li F, Raghothama KG, Bressan RA, Hasegawa PM, Pardo JM. 2009. The phosphate transporter PHT4;6 is a determinant of salt tolerance that is localized to the golgi apparatus of *Arabidopsis*. *Molecular Plant* **2**: 535–552.

Debaud JC, Gay G. 1987. *In vitro* fruiting under controlled conditions of the ectomycorrhizal fungus *Hebeloma cylindrosporum* associated with *Pinus pinaster*. *New Phytologist* **105**: 429–435.

Doré J, Kohler A, Dubost A, Hundley H, Singan V, Peng Y, Kuo A, Grigoriev IV, Martin F, Marmeisse R *et al.* 2017. The ectomycorrhizal basidiomycete *Hebeloma cylindrosporum* undergoes early waves of transcriptional reprogramming prior to symbiotic structures differentiation. *Environmental Microbiology* **19**: 1338–1354.

Doré J, Perraud M, Dieryckx C, Kohler A, Morin E, Henrissat B, Lindquist E, Zimmermann SD, Girard V, Kuo A *et al.* 2015. Comparative genomics, proteomics and transcriptomics give new insight into the exoproteome of the basidiomycete *Hebeloma cylindrosporum* and its involvement in ectomycorrhizal symbiosis. *New Phytologist* **208**: 1169–1187.

Fristedt U, Berhe A, Ensler K, Norling B, Persson BL. 1996. Isolation and characterization of membrane vesicles of *Saccharomyces cerevisiae* harboring the high-affinity phosphate transporter. *Archives of Biochemistry & Biophysics* **330**: 133–141.

Garcia K, Delaux P-M, Cope KR, Ané J-M. 2015. Molecular signals required for the establishment and maintenance of ectomycorrhizal symbiosis. *New Phytologist* **208**: 79–87.

Garcia K, Delteil A, Conéjéro G, Becquer A, Plassard C, Sentenac H, Zimmermann S. 2014. Potassium nutrition of ectomycorrhizal *Pinus pinaster*: overexpression of the *Hebeloma cylindrosporum Hc*Trk1 transporter affects the translocation of both K^+ and phosphorus in the host plant. *New Phytologist* **201**: 951–960.

Garcia K, Doidy J, Zimmermann SD, Wipf D, Courty P-E. 2016. Take a trip through the plant and fungal transportome of mycorrhiza. *Trends in Plant Science* **21**: 937–950.

Garcia K, Haider MZ, Delteil A, Corratgé-Faillie C, Conéjero G, Tatry M-V, Becquer A, Amenc L, Sentenac H, Plassard C *et al.* 2013. Promoter-dependent expression of the fungal transporter HcPT1.1 under Pi shortage and its spatial localization in ectomycorrhiza. *Fungal Genetics & Biology* **58–59**: 53–61.

Guo B, Jin Y, Wussler C, Blancaflor EB, Motes CM, Versaw WK. 2008. Functional analysis of the *Arabidopsis* PHT4 family of intracellular phosphate transporters. *New Phytologist* **177**: 889–898.

Hacquard S, Tisserant E, Brun A, Legue V, Martin F, Kohler A. 2013. Laser microdissection and microarray analysis of *Tuber melanosporum* ectomycorrhizas reveal functional heterogeneity between mantle and Hartig net compartments. *Environmental Microbiology* **15**: 1853–1869.

Harley JL. 1978. Ectomycorrhizas as nutrient absorbing organs. *Proceedings of the Royal Society of London. Series B: Biological Sciences* **203**: 1–21.

Harrison MJ, van Buuren ML. 1995. A phosphate transporter from the mycorrhizal fungus *Glomus versiforme*. *Nature* **378**: 626–629.

Hinsinger P. 2001. Bioavailability of soil inorganic P in the rhizosphere as affected by root induced chemical changes: a review. *Plant and Soil* **237**: 173–195.

Hürlimann HC, Pinson B, Stadler-Waibel M, Zeeman SC, Freimoser FM. 2009. The SPX domain of the yeast low-affinity phosphate transporter Pho90 regulates transport activity. *EMBO Report* **10**: 1003–1008.

Kariman K, Barker SJ, Jost R, Finnegan PM, Tibbett M. 2014. A novel plant–fungus symbiosis benefits the host without forming mycorrhizal structures. *New Phytologist* **201**: 1413–1422.

Kemppainen MJ, Pardo AG. 2010. pHg/pSILBAγ vector system for efficient gene silencing in homobasidiomycetes: optimization of ihpRNA – triggering in the mycorrhizal fungus *Laccaria bicolor*. *Microbial Biotechnology* **3**: 178–200.

Kohler A, Kuo A, Nagy LG, Morin E, Barry KW, Buscot F, Canback B, Choi C, Cichocki N, Clum A *et al.* 2015. Convergent losses of decay mechanisms and rapid turnover of symbiosis genes in mycorrhizal mutualists. *Nature Genetics* **47**: 410–415.

Legendre P, Legendre L. 1998. *Numerical ecology*, 2nd edn. Amsterdam, the Netherlands: Elsevier.

Loth-Pereda V, Orsini E, Courty P-E, Lota F, Kohler A, Diss L, Blaudez D, Chalot M, Nehls U, Bucher M *et al.* 2011. Structure and expression profile of the phosphate Pht1 transporter gene family in mycorrhizal *Populus trichocarpa*. *Plant Physiology* **156**: 2141–2154.

Martinez P, Persson B. 1998. Identification, cloning and charaterization of a derepressible Na^+-coupled phosphate transporter in *Saccharomyces cerevisiae*. *Molecular Genomics Genetics* **258**: 628–638.

Melin E, Nilsson H. 1950. Transfer of radioactive phosphorus to pine seedlings by means of mycorrhizal hyphae. *Physiologia Plantarum* **3**: 88–92.

Nehls U, Plassard C. 2018. Nitrogen and phosphate metabolism in ectomycorrhizas. *New Phytologist*. doi: 10.1111/nph.15257.

Ngari C, Combier J-P, Doré J, Marmeisse R, Gay G, Melayah D. 2009. The dominant *Hc.SdhR* carboxin-resistance gene of the ectomycorrhizal fungus *Hebeloma cylindrosporum* as a selectable marker for transformation. *Current Genetics* **55**: 223–231.

Norkrans B. 1949. Some mycorrhiza-forming *Tricholoma* species. *Svensk Botanisk Tidskrift* **43**: 485–490.

Ohno T, Zibilske LM. 1991. Determination of low concentrations of phosphorus in soil extracts using malachite green. *Soil Science Society of America Journal* **55**: 892–895.

Peters PJ, Bos E, Griekspoor A. 2006. Cryo-immunogold electron microscopy. *Current Protocols in Cell Biology* **32**: 4.7.1–4.7.19.

Plassard C, Barry D, Eltrop L, Mousain D. 1994. Nitrate uptake in maritime pine (*Pinus pinaster*) and the ectomycorrhizal fungus *Hebeloma cylindrosporum*: effect of ectomycorrhizal symbiosis. *Canadian Journal of Botany* **72**: 189–197.

Plassard C, Dell B. 2010. Phosphorus nutrition of mycorrhizal trees. *Tree Physiology* **30**: 1129–1139.

Plett JM, Yin H, Mewalal R, Hu R, Li T, Ranjan P, Jawdy S, De Paoli HC, Butler G, Burch-Smith TM *et al.* 2017. *Populus trichocarpa* encodes small, effector-like secreted proteins that are highly induced during mutualistic symbiosis. *Scientific Reports* **7**: 382.

Preuss CP, Huang CY, Gilliham M, Tyerman SD. 2010. Channel-like characteristics of the low-affinity barley phosphate transporter PHT1;6 when expressed in *Xenopus oocytes*. *Plant Physiology* **152**: 1431–1441.

Raghothama KG. 1999. Phosphate acquisition. *Annual Review of Plant Physiology and Plant Molecular Biology* **50**: 665–693.

Rao PS, Niederpruem DJ. 1969. Carbohydrate metabolism during morphogenesis of *Coprinus lagopus* (*sensu* Buller). *Journal of Bacteriology* **100**: 1222–1228.

R Development Core Team. 2004. *R: a language and environment for statistical computing*. Vienna, Austria: R Foundation for Statistical Computing.

Schott S, Valdebenito B, Bustos D, Gomez-Porras JL, Sharma T, Dreyer I. 2016. Cooperation through competition – dynamics and microeconomics of a minimal nutrient trade system in arbuscular mycorrhizal symbiosis. *Frontiers in Plant Science* **7**: 912.

Smith SE, Anderson IC, Smith FA. 2015. Mycorrhizal associations and phosphorus acquisition: from cells to ecosystems. *Annual Plant Reviews* **48**: 409–440.

Smith SE, Read DJ. 2008. *Mycorrhizal symbiosis*, 3rd edn. London, UK: Academic Press.

Solé VA, Papillon E, Cotte M, Walter Ph, Susini J. 2007. A multiplatform code for the analysis of energy-dispersive X-ray fluorescence spectra. *Spectrochimica Acta. Part B* **62**: 63–68.

Tatry M-V, El Kassis E, Lambilliotte R, Corratgé C, Van Aarle I, Amenc LK, Alary R, Zimmermann S, Sentenac H, Plassard C. 2009. Two differentially regulated phosphate transporters from the symbiotic fungus *Hebeloma cylindrosporum* and phosphorus acquisition by ectomycorrhizal *Pinus pinaster*. *Plant Journal* **57**: 1092–1102.

Torres-Aquino M, Becquer A, Le Guernevé C, Louche J, Amenc LK, Staunton S, Quiquampoix H, Plassard C. 2017. The host plant *Pinus pinaster* exerts specific effects on phosphate efflux and polyphosphate metabolism of the ectomycorrhizal fungus *Hebeloma cylindrosporum*: a radiotracer, cytological staining and ^{31}P NMR spectroscopy study. *Plant, Cell & Environment* **40**: 190–202.

Vance CP, Uhde-Stone C, Allan DL. 2003. Phosphorus acquisition and use: critical adaptations by plants for securing a nonrenewable resource. *New Phytologist* **157**: 423–447.

Vantelon D, Trcera N, Roy D, Moreno T, Mailly D, Guilet S, Metchalkov E, Delmotte F, Lassalle B, Lagarde P *et al.* 2016. The LUCIA beamline at SOLEIL. *Journal of Synchrotron Radiation* **23**: 635–640.

Wang J, Li T, Wu X, Zhao Z. 2014. Molecular cloning and functional analysis of a H^+ dependent phosphate transporter gene from the ectomycorrhizal fungus *Boletus edulis* in southwest China. *Fungal Biology* **118**: 453–461.

Wege S, Khan GA, Jung J-Y, Vogiatzaki E, Pradervand S, Aller I, Meyer AJ, Poirier Y. 2016. The EXS domain of PHO1 participates in the response of shoots to phosphate deficiency via a root-to-shoot signal. *Plant Physiology* **170**: 385–400.

Wild R, Gerasimaite R, Jung J-Y, Truffault V, Pavlovic I, Schmidt A, Saiardi A, Jessen HJ, Poirier Y, Hothorn M *et al.* 2016. Control of eukaryotic phosphate homeostasis by inositol polyphosphate sensor domains. *Science* **352**: 986–990.

Xie X, Lin H, Peng X, Xu C, Sun Z, Jiang K, Huang A, Wu X, Tang N, Salvioli A *et al.* 2016. Arbuscular mycorrhizal symbiosis requires a phosphate transceptor in the *Gigaspora margarita* fungal symbiont. *Molecular Plant* **9**: 1583–1608.

Ye JJ, Reizer J, Cui XW, Saier MH. 1994. ATP-dependent phosphorylation of serine-46 in the phosphocarrier protein HPr regulates lactose/H^+ symport in *Lactobacillus brevis*. *Proceedings of the National Academy of Sciences, USA* **91**: 3102–3106.

Zheng R, Wang J, Liu M, Duan G, Gao X, Bai S, Han Y. 2016. Molecular cloning and functional analysis of two phosphate transporter genes from *Rhizopogon luteolus* and *Leucocortinarius bulbiger*, two ectomycorrhizal fungi of *Pinus tabulaeformis*. *Mycorrhiza* **26**: 633–644.

Supporting Information

Additional supporting information may be found online in the Supporting Information section at the end of the article:

Fig. S1 Variation of fluorescence pixel intensity plotted from profiles traced over P X-ray fluorescence maps from *P. pinaster* root sections.

Fig. S2 Diagram of the binary vector constructed for overexpression of *H. cylindrosporum* genes.

Fig. S3 Specificity of the HcPT2 antibodies.

Fig. S4 Localization of HcPT2 by a translational fusion approach in *H. cylindrosporum* – *P. pinaster* ectomycorrhizas.

Fig. S5 Expression of *HcPT1.1* and *HcPT1.2* in *HcPT2*-silencing and *HcPT2*-overexpressing lines of *H. cylindrosporum* grown in pure culture.

Fig. S6 Development of symbiotic structures on *P. pinaster* roots colonized by wild-type (h7) and transgenic fungal strains (Ctl, RNAi-PT2-6, RNAi-PT2-9, OE-PT2-4 and OE-PT2-7).

Fig. S7 Total P accumulation in *P. pinaster* plants grown alone or in association with *H. cylindrosporum*.

Fig. S8 Growth and ^{32}Pi uptake of *HcPT2*-silencing and *HcPT2*-overexpressing lines of *H. cylindrosporum* grown in pure culture for ^{32}P experiments.

Fig. S9 Release of ^{32}Pi (in Bq per gram of fungal fresh weight) from *HcPT2*-silencing and *HcPT2*-overexpressing lines of *H. cylindrosporum* in the symbiotic interface-mimicking experiment.

Table S1 Primers used in this study

Methods S1 Full description of the methods used to run the X-ray fluorescence mapping and the ^{32}P labeling experiments, to assess the localization of HcPT2 proteins in ectomycorrhizal sections either using HcPT2-EGFP fusion protein or immunolocalization, and antibody specificity using western-blot analysis.

Please note: Wiley Blackwell are not responsible for the content or functionality of any Supporting Information supplied by the authors. Any queries (other than missing material) should be directed to the *New Phytologist* Central Office.